Biosensors and Bioelectronics 47 (2013) 467–474

Contents lists available at SciVerse ScienceDirect

Biosensors and Bioelectronics

journal homepage: www.elsevier.com/locate/bios

MultisHRP-DNA-coated CMWNTs as signal labels for an ultrasensitive hepatitis C virus core antigen electrochemical immunosensor

Cuixia Ma [a], Mo Liang [a], Li Wang [a], Hua Xiang [a], Yingtao Jiang [b], Yiyan Li [b], Guoming Xie [a,*]

[a] Key Laboratory of Medical Diagnostics of Ministry of Education, Department of Laboratory Medicine, Chongqing Medical University, Chongqing 400016, PR China

[b] Nevada Nanotechnology Center, College of Engineering, University of Nevada, Las Vegas, NV 89154-4026, USA

ARTICLE INFO

Article history:
Received 31 December 2012
Received in revised form
18 March 2013
Accepted 19 March 2013
Available online 6 April 2013

Keywords:
Graphitized mesoporous carbons
Methylene blue
Immunosensor
Carboxyl multi-wall carbon nanotubes
Hepatitis C virus core antigen

ABSTRACT

An ultrasensitive and selective electrochemical immunosensor was developed for the detection of hepatitis C virus (HCV) core antigen. The immunosensor consists of graphitized mesoporous carbon–methylene blue (GMCs–MB) nanocomposite as an electrode modified material and a horseradish peroxidase-DNA-coated carboxyl multi-wall carbon nanotubes (CMWNTs) as a secondary antibody layer. After modification of the electrode with GMCs–MB nanocomposite, Au nanoparticles were electrodeposited on to the electrode to immobilize the captured antibodies. The bridging probe and secondary antibodies linked to the CMWNTs, and DNA concatamers were obtained by hybridization of the biotin-tagged signal and auxiliary probes. Finally, streptavidin-horseradish peroxidases (HRP) were labeled on the secondary antibody layer via biotin-streptavidin system. The reduction current of MB were generated in the presence of hydrogen peroxide and monitored by square wave voltammetry. Under optimum conditions, the amperometric signal increased linearly with the core antigen concentration (0.25 pg mL^{-1} to 300 pg mL^{-1}). The immunosensor exhibites the detection limit as low as 0.01 pg mL^{-1} and it has a high selectivity. The new protocol showed acceptable stability and reproducibility, as well as favorable recovery for HCV core antigen in human serum. The proposed immunosensor has great potential for clinical applications.

1. Introduction

Hepatitis C virus (HCV) infection, which presents as persistent infection in up to 85% of all infected individuals (Patrizia et al., 2012), is a global health problem. Once HCV-infected patients develop cirrhosis or hepatocellular carcinoma, low cure rates and serious side effects shall be expected (Peter et al., 2012). That is why accurate and sensitive diagnosis of HCV in blood samples during the early stages of infection is so crucial. In the last decade, HCV core antigen levels have been suggested as potential markers for viral replication. HCV core antigen has been reported to appear earlier than anti-HCV antibody and may be detected within 1 or 2 days following the appearance of HCV RNA in serum (Laperche et al., 2005; Leary et al., 2006; Widell et al., 2002). Several studies have revealed significant correlations between HCV core antigen levels and HCV RNA levels in untreated patients with high viral loads (Park et al., 2010; Tillmann et al., 2005). A specific and sensitive method for the quantification of HCV core antigen using an enzyme-linked immunosorbent assay (ELISA) screening method has previously been reported (Aoyagi et al., 1999; Koray et al., 2011). However, while ELISA is relatively less expensive than an HCV RNA test, it presents some limitations. For example, the assay appears to have a higher limit of detection than the HCV RNA test (Medici et al., 2011). Thus, alternative methods with lower detection limits, higher sensitivity and selectivity, and faster responses must be further developed.

Many signal amplification strategies have been developed to achieve highly sensitive electrochemical immunosensing, including the application of various nanomaterials (Chen et al., 2012; Mao et al., 2012). Carbon nanotubes (CNTs) have been extensively used as immobilized substrates for the fabrication of biosensors because of their attractive mechanical, electronic, and chemical properties (Subramanian et al., 2012). Several researchers have focused on the ability of surface-confined CNTs to promote electron-transfer reactions in biosensing devices (Kenzo et al., 2007; Luo et al., 2005). CNTs can also be coated with high loads of enzymes and secondary antibodies for signal amplification in sandwich immunoassays (Wang et al., 2004). The superior physical and chemical properties of graphitized mesoporous carbons (GMCs), which include high specific surface areas, good electrical conductivity, excellent chemical stability, and large pore volumes, indicate their great potential application in electrochemical

* Corresponding author. Tel./fax: +86 23 68485240.
E-mail address: guomingxie@cqmu.edu.cn (G. Xie).

0956-5663/$ - see front matter © 2013 Elsevier B.V. All rights reserved.
http://dx.doi.org/10.1016/j.bios.2013.03.058

biosensors (Neimark et al., 2009; Liu et al., 2012). The three-dimensional ordered mesopores of GMCs provide more binding sites for biomacromolecules and help promote GMCs as favorable immobilization matrices. In addition, GMCs' excellent electrical conductivity can provide fast electron transfer for redox probe (Rajendiran and Annamalai, 2012). However, a major issue that limits the application of GMCs is the poor dispersion of the material in aqueous solution (Lu et al., 2009).

In this study, we attempt to prepare mixtures of GMCs in the presence of an appropriate ratio of sodium dodecyl sulfate (SDS) and chitosan (CS) to generate stable homogeneous dispersions. GMCs–methylene blue (MB) nanocomposites were obtained by attachment of MB to the GMCs to yield a modified electrode. Au nanoparticles (AuNPs) were then electrodeposited on this electrode to immobilize monoclonal HCV core antibody (Ab_1) as the primary antibody. To amplify electrochemical signals, a bridging

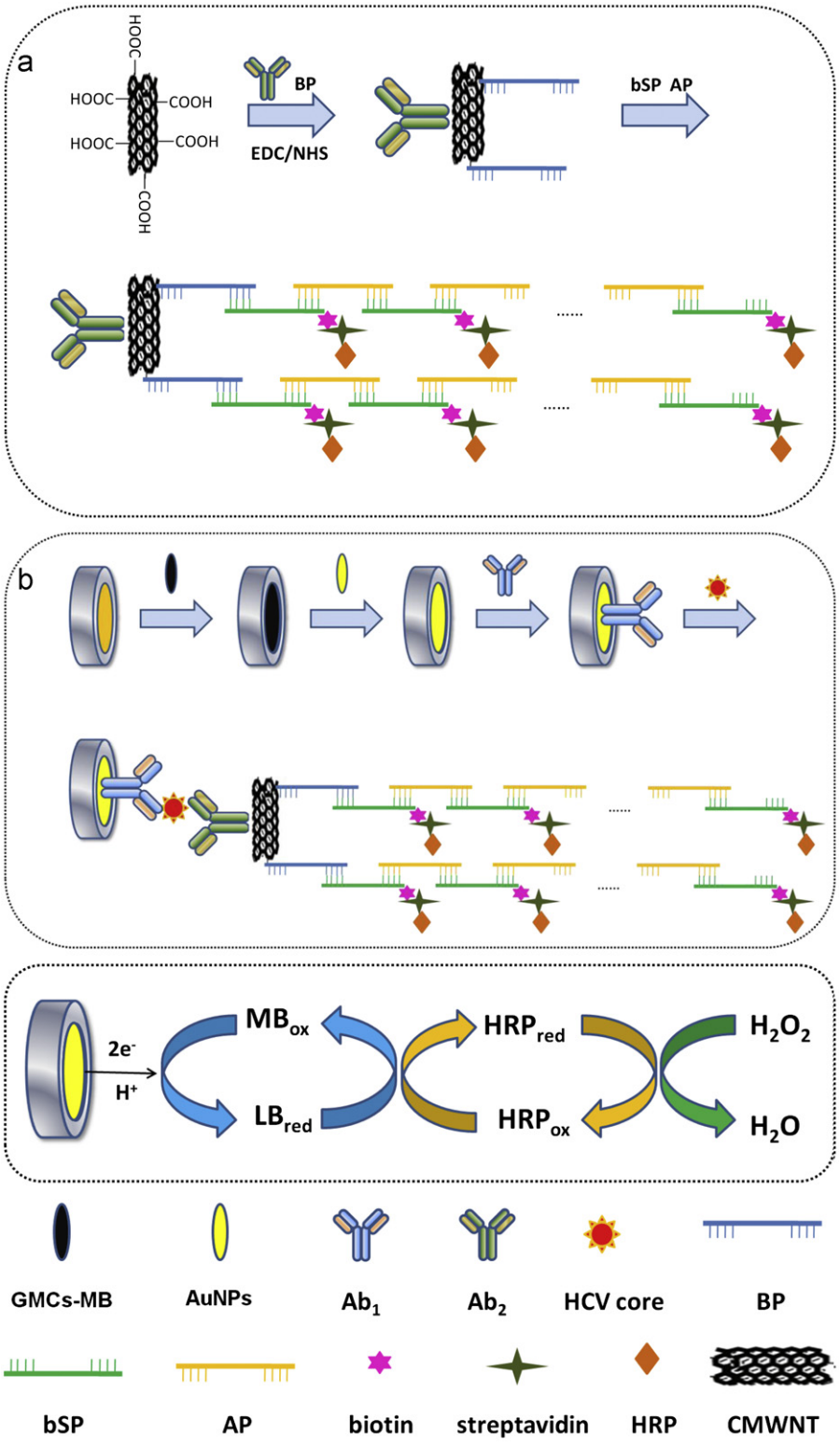

Scheme 1. (a) preparation of the multisHRP-DNA-CMWNTs-Ab_2bioconjugate; (b) fabrication procedure for the HCV immunosensor.

probe (BP) and secondary antibody were coated on CMWNTs. A biotin-tagged signal probe (bSP) and auxiliary probe (AP) were hybridized with the BP, and HRP were linked to the probes using biotin-streptavidin system as redox enzyme (see Scheme 1). MultisHRP-DNA-CMWNTs-labeled polyclonal HCV core antibody (Ab_2) serves as the secondary antibody that provides a large amount of redox enzyme and enables determination of detection signals despite very low analyte concentrations. Using HRP as a model enzyme and MB as effective electron mediator, the proposed immunosensor exhibites higher sensitivity, quicker response and lower detection limit compared with our previous research (Ma et al., 2012). This new approach possessed a great potential in low-cost and simple point-of-care of low-abundant biomarkers for clinical diagnostics.

2. Materials and methods

2.1. Materials and reagents

HCV core antigen, monoclonal HCV core antibody (Ab_1) and polyclonal HCV core antibody (Ab_2) were obtained from ViroStat, Inc. (Portland, USA). Bovine serum albumin (BSA, 96% to 99%), chloroauric acid ($HAuCl_4 \cdot 4H_2O$), H_2O_2 (30% w/v solution), *N*-hydroxysuccinimide (NHS), 1-ethyl-3-3(3-dimethylaminopropyl) carbodiimide (EDC), MB hydrate, Mecatohexanol (MCH) and GMCs (spherical diameter: 330 nm, average pore diameter: 137) were purchased from Sigma-Aldrich (St. Louis, MO, USA). SDS, tris–(hydroxymethyl) aminomethane, chitosan and streptavidin-HRP were obtained from Shanghai Sangon Biological Engineering Technology & Services Co., Ltd. (Shanghai, China). CMWNTs were purchased from Chengdu Organic Chemicals Co., Ltd. (Chengdu, China). All oligonucleotide sequences were synthesized by Shanghai Sangon Biological Engineering Technology & Services Co., Ltd.; these sequences are listed in Table. S1.

2.2. Instrumentation

All electrochemical experiments were carried out using a CHI 660D electrochemical work station (Shanghai Chenhua Instruments, China). A conventional three-compartment electrochemical cell was employed in all electrochemical measurement. The workstation employed a modified Au electrode as a working electrode, a KCl-saturated Ag/AgCl electrode as reference electrode and a Pt wire as an auxiliary electrode. GMCs morphologies were investigated by transmission electron microscopy (TEM) using an H-7500 electron microscope (Hitachi, Japan). A Nova 400 field emission scanning electron microscope (SEM) (FEI Nova-400, USA) and NanoWizard II (JPK Instruments Inc., Germany) atomic force microscope (AFM) were used to observe images of the CMWNTs and multisHRP-DNA-CMWNTs-Ab_2.

Preparation of the homogeneous GMCs–MB suspension

A 0.5 wt% CS solution was prepared by dissolving 150 mg of chitosan powder in 30 mL of 1.0% (v/v) acetic acid solution and then stirred for 2 h at room temperature until completely dispersed. This CS solution was added to an aqueous solution of SDS (1.5 g of SDS powder in 100 mL of dilute aqueous HCl) under stirring to obtain a uniform SDS–CS mixture. The CS volume added to the SDS solution was optimized. GMCs (5.0 mg) were subsequently dispersed into the SDS–CS solution for 1 h with ultrasonication to form a homogeneous GMC suspension. MB solution (5 mM) was added to the GMC suspension, and stirring was performed for 2 h. GMCs–MB composites were subsequently obtained.

2.3. Preparation of multisHRP-DNA-CMWNTs-Ab_2 bioconjugates

DNA-CMWNTs-Ab_2 nanocomposites were synthesized according to a previous report with slight modification (Li et al., 2012; Wan et al., 2011). The BP and Ab_2 were attached to the broken tips of CMWNTs containing carboxylic acid groups using the coupling agents, EDC and NHS, by formation of amide linkages between the amine groups of BP and Ab_2 and the carboxylic acid groups of the CMWNTs. Briefly: 1 mg of CMWNTs was dispersed into 1 mL of 0.01 M 2-(*N*-morpholino)ethanesulfonic acid buffer (MES buffer, pH 7.0). This mixture was sonicated at room temperature until a homogeneous solution was obtained. About 1 mL of 400 mM EDC and 100 mM NHS solution were then added to the mixture and stirring was continued for another hour. After centrifugation, 150 μL of 100 μM BP and 50 μL of 15 μg mL^{-1} Ab_2 were added to the resulting pellet and stirred overnight at room temperature. The reaction mixture was subsequently centrifuged at 5000 rpm and 4 °C for 10 min, and the precipitate obtained was washed three times with phosphate buffer solution (PBS, pH 7.2) to remove the free BP and Ab_2. The hybridization experiment was carried out using the synthetic oligonucleotides bSP and AP. MCH (1 mM) was added to the CMWNTs-Ab_2-BP for 30 min to block nonspecific BP binding sites, after which the mixture was resuspended in 500 μL of Tris–HCl buffer (pH 7.4). Approximately 100 μM bSP and 100 μM AP were added to the suspension with gentle stirring at 37 °C for 30 min. Washing with Tris–HCl buffer followed to eliminate non-specific absorbed DNA. Finally, DNA-CMWNTs-Ab_2 nanocomposites were obtained.

Exactly 100 μL of sHRP was mixed with the DNA-CMWNTs-Ab_2 nanocomposites. Incubation of the mixture for 40 min at 37 °C followed. The product was then centrifuged at 5000 rpm for 20 min at 4 °C. The bioconjugated precipitates obtained were resuspended in 1 mL of 0.05% Tween-20 in PBS (pH 7.2) to form a homogeneous dispersion and then stored in a refrigerator at 4 °C. The multisHRP-DNA-CMWNTs-Ab_2 bioconjugates obtained were diluted with 0.1% BSA in PBS immediately before use. HRP-CMWNTs-Ab_2 and CMWNTs-Ab_2 nanocomposites were also synthesized as controls using the same EDC/NHS amidization protocol.

2.4. Assembly of the electrochemical immunosensor

The stepwise procedure for the fabrication of the HCV immunosensor is illustrated in Scheme 1b. Prior to immobilization, each Au electrode (3 mm in diameter) was polished with 1.0, 0.3, and 0.05 μm alumina slurry in sequence and then washed ultrasonically in double distilled water and ethanol for 15 min. Each electrode was then subjected to electrochemical pretreatment of 5 cyclic potential scans between 0.0 and 1.5 V at 100 mVs^{-1} in 0.5 M H_2SO_4. About 5 μL of the as-prepared GMCs–MB suspension was dropped onto the clean Au electrodes, which were then dried in a desiccator. The GMCs–MB/Au electrode was immersed into 1% $HAuCl_4$ solution, and electrodeposition was performed by cyclic voltammetry at −0.66 V for 200 s to obtain the AuNPs/GMCs–MB-modified electrode. Approximately 5 μL of a 30 μg mL^{-1} Ab_1 solution in PBS was dropped onto the AuNPs/GMCs–MB/Au electrode. The Ab_1/AuNPs/GMCs–MB/Au electrode was then left to stand overnight. About 5 μL of a 0.25% BSA blocking solution was subsequently deposited onto the Ab_1/AuNPs/GMCs–MB/Au, followed by incubation for 40 min. After rinsing thoroughly with 0.01 M PBS (pH 7.0), the immunosensor obtained was stored at 4 °C prior to electrochemical detection.

2.5. Measurement procedure

Electrochemical measurements of the immunosensor toward the HCV core antigen samples or standards were carried out using

a sandwich-type immunoassay format with multisHRP-DNA-CMWNTs-Ab_2 as the secondary antibody and H_2O_2 as the enzyme substrate. Different core antigen concentrations were tested in this experiment, and each antigen concentration was tested with a separate electrode. Briefly: The immunosensor was placed in an incubation solution containing various concentrations of HCV core antigen for 30 min at 37 °C and then washed extensively with distilled water to remove unbound HCV core antigen molecules. The resulting substrates were subsequently submerged in another incubation solution containing multisHRP-DNA-CMWNTs-Ab_2 for 30 min at 37 °C. After rinsing thoroughly with distilled water, electrochemical measurement was performed in PBS (pH 7.0) containing 0.5 mM H_2O_2. The peak current of MB was measured using square wave voltammetry (SWV). The SWV peak currents obtained were registered and plotted against known HCV core antigen concentrations to obtain a calibration curve.

2.6. Sample preparation

Samples were prepared using HCV core antigen standard solutions of different concentrations. All of the fresh human specimens used in this study were granted by the First Affiliated Hospital, Chongqing Medical University and the First People's Hospital, Jiulongpo District of Chongqing.

3. Results and discussion

3.1. Characterization

3.1.1. SEM and AFM characterization

Field-emission SEM was used for characterization. Fig. 1a and b shows SEM images of the CMWNTs and multisHRP-DNA-CMWNTs-Ab_2, respectively. The surface of the multisHRP-DNA-CMWNTs-Ab_2 was rougher than that of the CMWNTs. This roughness may be attributed to the loading of oligonucleotides and HCV antibodies on the electrode. Fig. 1c shows numerous spherical AuNPs with an average diameter of 50 nm electrodeposited on the surface of the GMCs–MB nanocomposite film, revealing the grainy structures of the electrode surface. AFM was also utilized to probe the attachment of DNA and Ab_2 to the CMWNTs. A three-dimensional height map displays AFM images of the CMWNTs and multisHRP-DNA-CMWNTs-Ab_2, as shown in Fig. 1d and e. CMWNTs with a dense, spiky appearance may be observed in

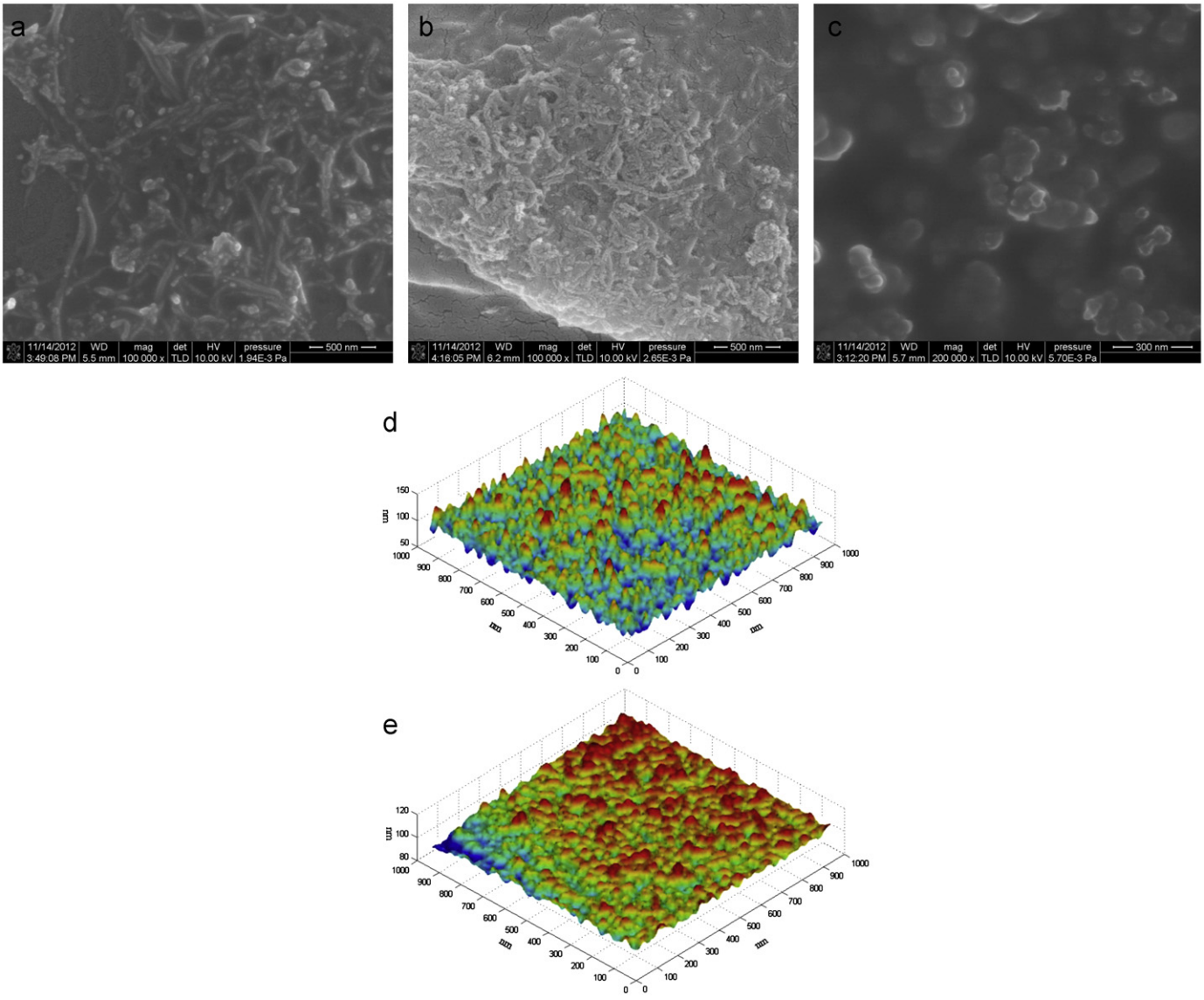

Fig. 1. SEM images of (a) CMWNTs, (b) multisHRP-DNA-CMWNTs-Ab_2 and (c) AuNPs.AFMimages of (d) CMWNTs and (e) multisHRP-DNA-CMWNTs-Ab_2.

Fig. 1d. After the antibodies and oligonucleotides had been covalently linked onto the CMWNTs using EDC/NHS, the spiky nanotube features disappeared and the nanoparticles showed a blunt appearance, as can be observed in Fig. 1e.

3.1.2. Cyclic voltammetric characterization

Cyclic voltammetry (CV) is an effective and convenient technique for detecting the current response of analytes in electrochemical determination (Yuan et al., 2012). Fig. 2 shows the cyclic voltammograms obtained from the modified electrodes in PBS (pH 7.0) containing 0.1 M KCl and 5 mM $Fe(CN)_6^{3-/4-}$ at a scan rate of 50 mVs^{-1}. A reversible electrochemical response and a pair of well-defined redox peaks can be observed from the bare Au electrode (Fig. 2a). The peaks obtained may be attributed to the redox behaviors of [$Fe(CN)_6^{3-/4-}$]. The electron transfer ability of [$Fe(CN)_6^{3-/4-}$] may be improved by modification of the GMCs–SDS–CS composites, as evidenced by the increase in voltammetric responses of [$Fe(CN)_6^{3-/4-}$] on the GMCs–MB modified electrode (Fig. 2b). After deposition of Au nanoparticles on the modified electrode, the highest redox peaks were obtained, with anodic and cathodic peak potentials of 0.28 V and 0.13 V, respectively (peak potential difference of 150 mV) (Fig. 2c). AuNPs on the GMCs–MB film significantly influenced the improvement in electron transfer between [$Fe(CN)_6^{3-/4-}$] and the electrode. Immobilization of the captured antibodies on the electrode surface induced a large decrease in peak current (Fig. 2d), indicating that the captured antibodies were successfully immobilized on the electrode surface. The peak current further decreased after using a BSA blocking solution to block non-specific binding site (Fig. 2e). When the HCV core antigen was captured by its antibody, the electron transfer of ferricyanide to the electrode surface was further hindered (Fig. 2f). The peak current increased after immobilization of CMWNTs-Ab_2 on the electrode surface (Fig. 2g), which is may be due to the excellent electronic conductivity of the CMWNTs.

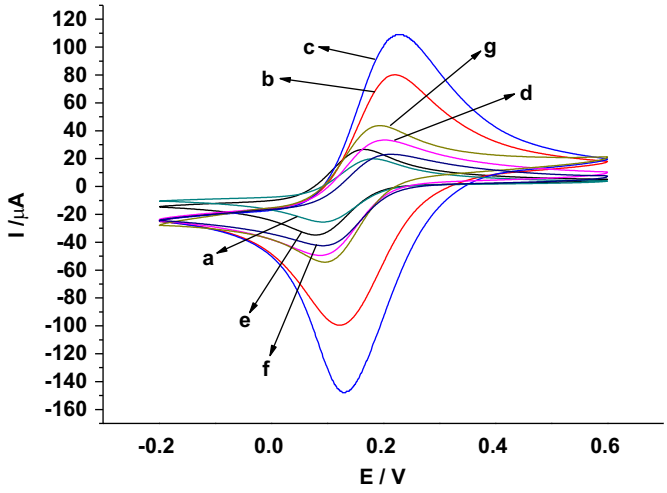

Fig. 2. Cyclic voltammograms of the surface-functionalized Au electrodes in pH 7.0 phosphate buffer solution containing 5 mM $Fe(CN)_6^{3-/4-}$ and 0.1 M KCl at a scan rate of 50 mV s^{-1}: (a) bare Au electrode; (b) GMCs–MB/Au; (c) AuNPs/GMCs–MB/Au; (d) Ab_1/AuNPs/GMCs–MB/Au; (e) BSA/Ab_1/AuNPs/GMCs–MB/Au; (f)core antigen/Ab_1/AuNPs/GMCs–MB/Au; (g) CMWNTs-Ab_2/core antigen /Ab_1/AuNPs/ GMCs–MB/Au.

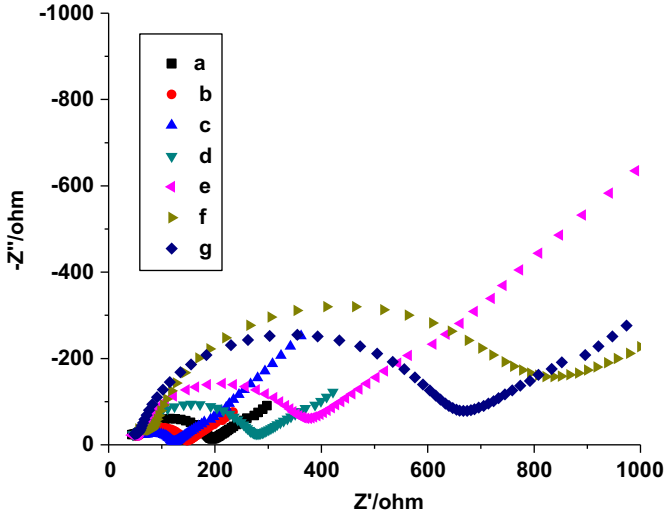

Fig. 3. The EISspectra for each immobilization step:(a) bare Au electrode; (b) GMCs–MB/Au; (c) AuNPs/GMCs–MB/Au; (d) Ab_1/AuNPs/GMCs–MB/Au; (e) BSA/Ab_1/AuNPs/GMCs–MB/Au; (f) core antigen/Ab_1/AuNPs/GMCs–MB/Au; (g) CMWNTs-Ab_2/\core antigen/Ab_1/AuNPs/GMCs–MB/Au. The reaction solution is PBS(pH7.0) containing 5 mM$Fe(CN)_6^{3-/4-}$ and 0.1 M KCl.

3.1.3. Electrochemical impedance spectroscopy characterization

The features of the surface-modified Au electrode were also monitored by EIS experiments. Fig. 3 shows significant differences in the electron transfer resistance (Ret) obtained from every surface modification step. Compared with the bare Au electrode (Fig. 3a), the diameter of the semicircular element, which corresponds to Ret on the electrode surface, decreased when the GMCs–MB film was covered (Fig. 3b). After AuNPs were electrodeposited on the GMCs–MB film, the semicircular diameter further decreased (Fig. 3c), thus confirming that AuNPs promote electron exchange between [$Fe(CN)_6$]$^{3-/4-}$ and the electrode. An insulating layer functioning as a barrier to interfacial electron transfer was generated by the primary antibody. This result is reflected by the increase in diameter of the semicircular portion of the spectrum (Fig. 3d). Further increases in the semicircular diameter of the impedance spectrum were observed when the modified electrode was incubated in BSA solution, as shown in Fig. 3e. Incubation of the HCV core resulted in an obvious increase in the interface impedance (Fig. 3f), indicating that a specific reaction was generated between the antigen and the antibody. When CMWNTs-Ab_2 was incubated with the core antigen/Ab_1/AuNPs/GMCs–MB/Au, a smaller Ret was observed (Fig. 3g). This result indicates that the CMWNTs-Ab_2-modified electrode features an excellent conductive interface. These data are consistent with the results obtained from the CV experiments.

3.2. Optimization of analytical conditions

3.2.1. Optimization of the CS volume

Different volumes (100, 200, 300, 400, 500 μL) of 0.5 wt% CS added to 1 mL of GMCs–MB composites were prepared. TEM images show the different dispersion degree of GMCs–MB. No obvious differences were observed from Fig. S1a, b, and c. The GMCs–MB nanocomposites presented a homogenous dispersion in SDS–CS solutions with 100, 200, and 300 μL of CS. However, the GMCs–MB nanocomposites aggregated with further increases in CS volume (Fig. S1d and e), indicating that CS influences the dispersion of GMCs–MB in the SDS solution. SDS cannot efficiently form films on the electrode surface. No apparent GMCs–MB nanocomposite film was formed on the electrodes when small volumes of CS were utilized (100 and 200 μL), as shown in Fig. S1f. Excellent film-forming ability and favorable dispersion of GMCs–MB nanocomposites were obtained simultaneously when the CS volume applied was 300 μL.

3.2.2. Effect of the ratio of Ab_2 to BP

The optimal ratio of Ab_2 to BP was investigated to improve the signal amplification of the developed immunosensor. Five HCV

immunosensors with different Ab_2:BP ratios (1:20; 1:40; 1:60; 1:80; 1:100) were used to detect 200 pg mL^{-1} HCV core antigen. The largest peak current was obtained when the ratio was 1:60, as shown in Fig. S2. When the ratio was increased from 1:20 to 1:60, larger amounts of BP attached to the CMWNTs, larger amounts of HRP were linked, and higher sensitivity of the electrochemical immunosensor was observed. The current response decreased with further increases in Ab_2:BP ratio up to 1:100. This decrease observed may be attributed to two factors: (i) steric hindrance may result in a decrease in electrochemical signals if the amount of BP on the CMWNTs surface is too large and (ii) more BP molecules occupy the CMWNTs surface area, thereby limiting the binding of Ab_2 on the CMWNTs and decreasing the signal labels (multisHRP-DNA-CMWNTs-Ab_2) on the electrode surface. The optimal Ab_2:BP ratio for signal amplification was determined as 1:60.

3.2.3. Optimization of experiment parameters

The sensor was incubated in 200 pg mL^{-1} HCV core antigen solution for different times at room temperature to examine the influence of incubation time on the current response of the sensor. The current response increased with increasing incubation time and then reached a plateau at 25 min. Thus, an incubation time of 25 min was chosen as the optimal time for further experiments.

The dependence of the biosensor response on the pH of the measurement solution was investigated at pH values ranging from 3.0 to 9.0 and in the presence of H_2O_2. The current response increased sharply from pH 3.0 to 7.0, achieved maximum values at pH 7.0, and then decreased from pH 7.0 to 9.0 (Fig. S3B). Therefore, a solution pH of 7.0 was selected for further experiments, similar to the optimum observed for soluble peroxidase (Ni et al., 2012). The effect of pH of the working solution was determined by recording the square wave voltammograms of the HCV core antigen at each pH. The maximal SWV current was achieved at pH 7.0.

The effect of incubation time of sHRP on the performance of the electrochemical HCV immunosensor is demonstrated in Fig. S3C. Electrochemical responses obtained at different incubation times (10, 20, 30, 40, 50, 60 min) were recorded. The responses reached a plateau when the incubation time was 40 min, likely because the bSP sites that are linked to sHRP reached saturation.

MB concentration was also optimized in the experiment. Different MB concentrations were added to GMCs suspensions and the obtained electrodes were used to detect 200 pg mL^{-1} HCV core antigens. Data in Fig. S3D indicate that the maximum signal is achieved for MB concentrations equal or higher than 5 mM.

3.3. Comparison of the proposed protocol with a control experiment

Two sets of control experiments, including a multisHRP-DNA-free immunosensor and a DNA-free immunosensor, were performed to further test the proposed immunosensing principle (Fig. S4). In the first experiment, biosensors constructed with Ab_2 alone were used to measure 200 pg mL^{-1} HCV core antigen in PBS with H_2O_2. As expected, the signals from these control biosensors were not significant due to the absence of multisHRP (Fig. S4a). The purpose of the second control experiment was to establish whether or not the DNA has an important role in the signal amplification of the immunosensor. The immunosensor without DNA displayed lower signal responses (Fig. S4b) compared with the experimental immunosensor (Fig. S4c). This result may be attributed to the fact that DNA provides a large number of sites to link with HRP, which significantly enhances detection signals.

In order to test that MB can efficiently shuttle electrons between the gold electrode and HRP labels, the cyclic voltammograms comparison was performed. Fig. S5 showed the MB response current change in the absence (blue line) and presence (black line) of H_2O_2. As we can see that the significant changes in the CV were detected with H_2O_2 presence. Electrocatalytic cycle can explain the principle of the changes in the experiment (Mucelli et al., 2008; Zamuner et al., 2008).

3.4. Analytical characteristics for HCV core antigen determination

Analytical calibrations for the HCV core antigen were performed by SWV under the optimized conditions determined previously. Fig. 4A shows increases in well-defined SWV responses with increasing HCV core antigen concentration (0.25 pg mL^{-1} to 300 pg mL^{-1}). Fig. 4B shows a good linear relationship between the change in cathodic peak currents obtained by SWV and the logarithm of different concentrations of HCV core antigen. Each point of the calibration graph corresponds to the mean value obtained from 5 independent measurements, and the error bars show the standard deviations of the measurements. The linear regression equation was I (μA) = 120.5+355.5 log C [pg mL^{-1}], with

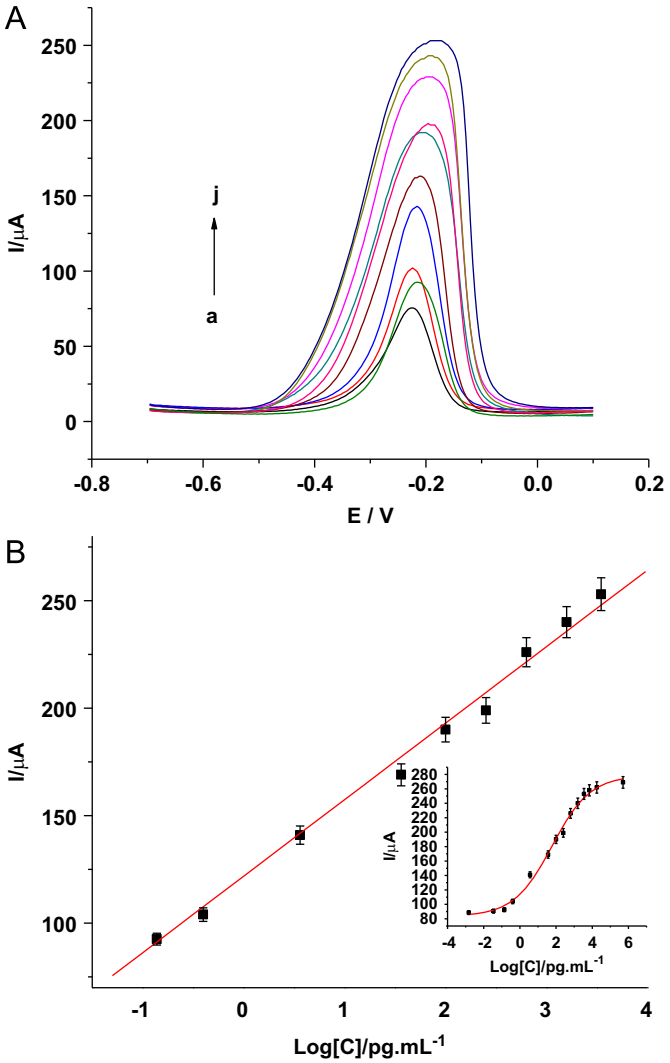

Fig. 4. (A) Incremental SWV responses of the immunosensor with increasing concentrations of HCV core antigen (from a to j: 0, 0.25, 0.5, 2.5, 12.5, 25, 50, 100, 200, and 300 pg mL^{-1}). (B) Calibration curve of the peak current response versus the logarithm of HCV core antigen concentration. The relative standard deviations (RSD) was 5.2%. The parameters of SWV are as follows: initial potential, −0.7 V; final potential, 0.1 V; amplitude, 25 mV; scan increment, 4 mV; and frequency, 25 Hz.

Table 1
Recovery studies of HCV core antigen from human serum samples.

Sample No.	Ag in serum (pg mL^{-1})	Ag added (pg mL^{-1})	Ag detected (pg Ml^{-1})	R%	RSD%
1	0	12.5	13.2	105.6	3.2
2	0	25	23.7	94.8	4.6
3	0	50	50.8	101.6	3.0
4	0	200	199.6	99.8	5.3

Ag, HCV core antigen, R%, recovery percentage, RSD%, relative standard deviation percentage.

a detection limit (LOD) of 0.01 pg mL^{-1} ($S/N=3$). The formulae used for LOD is LOD=3S/355.5 (S: the standard deviation of the 20 times of the background signal). The developed immunosensor presented favorable relevance in the range of 0.25 pg mL^{-1} to 300 pg mL^{-1} ($R=0.997$), which is much wider compared with reported immunosensors that use multi-enzyme systems (Lu et al., 2012; Kong et al., 2011). The insert in Fig. 4B shows that deviation from linearity is observed for antigen concentrations <0.25 pg mL^{-1} or >300 pg mL^{-1}.

The performance of the proposed electrochemical immunosensor was compared with other methods, including electrochemiluminescene, surface plasmon resonance, and immunochromatography, as shown in Table S2. The developed immunosensor showed a wider linear range and lower detection limit compared with these methods.

3.5. Cross-reactivity and recovery

The cross-reactivity was evaluated by comparing the SWV current at the immunosensor incubated with target analyte and other possible interfering agents in human serum, such as HCV NS5a, HBV surface antigen (HBsAg), HIV, and immunoglobulin G (IgG). When the immunosensor was incubated in 200 pg mL^{-1} pure HCV core antigen and the same solution containing interfering substances at 1 ng mL^{-1}, no obvious differences in signal currents were observed between treatments, as shown in Fig. S6. When the interfering agents were incubated with the sensor individually, the electrochemical signals obtained were almost identical to those obtained in the blank experiment. It indicated that these peaks corresponded to non-specific adsorption of HCV core antibody and that none of the species investigated interfered significantly on the immunosensor response.

A recovery test was performed to investigate the feasibility of the immunosensor for clinical applications. The analytical results for the human serum samples spiked with different concentrations of HCV core antigen are given in Table 1. The recovery values ranged from 94.8% to 105.6%. This result demonstrates that the developed immunosensor has potential clinical applicability for the detection of HCV core antigen.

3.6. Stability, reproducibility, repeatability, and regeneration of the immunosensor

In this study, the stability of the immunosensor was investigated. When the immunosensor was stored in the refrigerator at 4 °C for 10 d, 91.6% of the initial response was retained. This result suggests that the immunosensor has good stability.

The intra- and inter-assay coefficients of variation of the sensor were investigated to evaluate the reproducibility and repeatability of the immunosensor for HCV core antigen. Four concentrations of HCV core antigen (0.5, 12.5, 50, 200 pg mL^{-1}) were analyzed five times per determination within 10 h, and intra-assay coefficients of variation of 3.6%, 4.1%, 3.5%, and 5.3%, respectively, were obtained. Inter-assay coefficients of variation were evaluated by analyzing five immunosensors at 0.5, 12.5, 50, and 200 pg mL^{-1} HCV core antigen, and values of 2.8%, 3.2%, 5.4% and 3.8%, respectively, were obtained. This result suggests that the immunosensor has acceptable precision and reproducibility.

Regeneration is also a key factor in immunosensor development. Based on the reversibility of an immunoreaction, the immunosensor can be regenerated by immersion into an 8 M urea solution after the completion of each assay followed by washing with double distilled water to dissociate the antigen–antibody complex. The immunosensor retained 86% of its original current after five cycles of regeneration, and the relative standard deviation (RSD) was 3.1%.

4. Conclusion

An electrochemical immunosensor was developed for the ultrasensitive determination of HCV core antigen using multisHRP-DNA for signal amplification. The as-prepared immunosensor is composed of redox active GMCs–MB nanocomposites and signal amplified multisHRP-DNA-CMWNTs and exhibited a broad dynamic range and low detection limit. Extraordinary signal enhancement was achieved by DNA hybridization technology. The proposed method provides a promising universal multisHRP-DNA-CMWNTs label for different analytes. Future work will focus on the application of this immunosensor to other target analytes and biomarker types.

Acknowledgments

This work was financially supported by the Natural Science Research Foundation of China (81171415).

Appendix A. Supporting information

Supplementary data associated with this article can be found in the online version at http://dx.doi.org/10.1016/j.bios.2013.03.058.

References

Aoyagi, K., Ohue, C., Iida, K., Kimura, T., Tanaka, E., Kiyosawa, K., Yagi, S., 1999. Journal of Clinical Microbiology 37, 1802–1808.
Chen, H., Tang, D., Zhang, B., Liu, B., Cui, Y., Chen, G., 2012. Talanta 91, 95–102.
Kenzo, M., Taiji, K., Kagan, K., Yuzuru, T., Kazuhiko, M., Eiichi, T., 2007. Analytical Chemistry 79, 782–787.
Kong, F.Y., Zhu, X., Xu, M.T., Xua, J.J., Chen, H.Y., 2011. Electrochimica Acta 56, 9386–9390.
Koray, E., Burçin, Ş., Alpaslan, A., Jale, K., Gülşen, H., 2011. Diagnostic Microbiology Infectious Disease 70, 486–491.
Laperche, S., Marrec, N.L., Girault, A., Bouchardeau, F., Servant-Delmas, A., Maniez-Montreuil, M., Gallian, P., Levayer, T., Morel, P., Simon, N., 2005. Journal Clinical Microbiology 43, 3877–3883.
Leary, T.P., Gutierrez, R.A., Muerhoff, A.S., Birkenmeyer, L.G., Desai, S.M., Dawson, G. J., 2006. Journal of Medical Virology 78, 1436–1440.
Li, Y., Zhong, Z., Chai, Y., Song, Z., Zhuo, Y., Su, H., Liu, S., Wang, D., Yuan, R., 2012. Chemical Communication 48, 537–539.
Liu, B., Lu, L., Hua, E., Jiang, S., Xie, G., 2012. Microchimica Acta 178, 163–170.
Lu, X., Xiao, Y., Lei, Z., Chen, J., 2009. Biosensors and Bioelectronics 25, 244–247.
Lu, L., Liu, B., Zhao, Z., Ma, C., Luo, P., Liu, C., Xie, G., 2012. Biosensors and Bioelectronics 33, 216–221.
Luo, X.L., Xu, J.J., Wang, J.L., Chen, H.Y., 2005. Chemical Communication 16, 2169–2171.
Ma, C., Xie, G., Zhang, W., Liang, M., Liu, B., Xiang, H., 2012. Microchimica Acta 178, 331–340.
Mao, K., Wu, D., Li, Y., Ma, H., Ni, Z., Yu, H., Luo, C., Wei, Q., Du, B., 2012. Analytical Biochemistry 422, 22–27.
Medici, M.C., Furlini, G., Rodella, A., Fuertes, A., Monachetti, A., Calderaro, A., Galli, S., Terlenghi, L., Olivares, M., Bagnarelli, P., Costantini, A., DeConto, F., Sainz, M., Galli, C., Manca, N., Landini, M.P., Dettori, G., Chezzi, C., 2011. Journal of Clinical Virology 51, 264–269.
Mucelli, S.P., Zamuner, M., Tormen, M., Stanta, G., Ugo, P., 2008. Biosensors and Bioelectronics 23, 1900–1903.

Neimark, A.V., Lin, Y., Ravikovitch, P.I., Thommes, M., 2009. Carbon 47, 1617–1628.
Ni, Y., Wang, Y., Zhang, G., Shen, J., Zhao, W., Huang, X., 2012. Electrochimica Acta 69, 282–286.
Patrizia, F., Kurt, W., Harvey, A., 2012. Journal of Acquired Immune Deficiency Syndrome 59, 68.
Park, Y., Lee, J.H., Kim, B.S., Kimdo, Y., Han, K.H., Kim, H.S., 2010. Journal of Clinical Microbiology 48, 2253–2256.
Peter, Ferenci, 2010. Nature Reviews Gastroenterology and Hepatology 7, 191–193.
Rajendiran, T., Annamalai, S.K., 2012. Journal of Solid State Electrochemistry 16, 3861–3868.
Subramanian, V., Chinnakkaruppanan, R., Ja-an, A.H., 2012. Talanta 94, 315–319.
Tillmann, H.L., Wiegand, J., Glomb, I., Jelineck, A., Picchio, G., Wedemeyer, H., Manns, M.P., 2005. Zeitschrift fur Gastroenterologie 43, 11–16.
Wan, Y., Deng, W., Su, Y., Zhu, X., Peng, C., Hu, H., Peng, H., Song, S., Fan, C., 2011. Biosensors and Bioelectronics 30, 93–99.
Wang, J., Liu, G., Jan, M.R., 2004. Journal of American Chemical Society 126, 3010–3011.
Widell, A., Molnegren, V., Pieksma, F., Calmann, M., Peterson, J., Lee, S.R., 2002. Transfusion Medicine 12, 107–113.
Yuan, L., Wei, W., Liu, S., 2012. Biosensors and Bioelectronics 38, 79–85.
Zamuner, M., Mucelli, S.P., Tormen, M., Stanta, G., Ugo, P., 2008. European Journal of Nanomedicine 1, 33–36.